Incidence of Lead Uptake on the Microstructure of a (Mg, Ca)-Bentonite (Prrenjas, Albania)

Nevila Jozja, Patrick Baillif, Jean-Claude Touray, Fabrice Muller, Christian Clinard

1. Nevila Jozja
Address: Institut des Sciences de la Terre d'Orleans (Université d'Orléans) Rue de Saint-Amand, Bâtiment Géosciences, BP 6759, 45067 Orléans Cedex 2
Tel.: + 33 (0)6 12 65 63 35
Fax: +33 (0)2 38 41 70 46
e-mail: njozja@yahoo.com

2. Patrick Baillif
Address: Institut des Sciences de la Terre d'Orleans (Université d'Orléans) Rue de Saint-Amand, Bâtiment Géosciences, BP 6759, 45067 Orléans Cedex 2
Tel.: + 33 (0)2 38 41 72 26
Fax: + 33 (0)2 38 41 73 08
e-mail:patrick.baillif@univ-orleans.fr

Key words : lead, bentonite, microstructure, adsorption, cation exchange, XPS, TEM

Abstract

The article addresses Pb uptake and microstructural/morphological modifications of a (Mg, Ca) bentonite (Prrenjas, Albania) after interaction with solutions of elevated lead content. Comparison is made with a Wyoming montmorillonite transformed to the Mg-dominated form.

Characterized by X-ray diffraction (XRD) and Transmission Electron Microscopy (TEM) the Prrenjas bentonite is predominantly a smectite, containing 10% of interlayered illite, with associated kaolinite, antigorite, halloysite and minor chlorite. Significant magnesium is present in the octahedral layer in association with aluminium and iron. The CEC is rather high (above 80 meq/100g). Magnesium and calcium are the main cations exchanged during CEC determinations and Pb uptake experiments. From TEM studies, microstructural units are composed by closely packed clay particles with 10 to15 stacked platelets, in contrast with Wyoming montmorillonite.

Exchange experiments with lead nitrate on suspended clays, have been performed with concentrations ranging from 10^{-5} M to 10^{-2} M. A comparable capacity of lead sorption is observed by Atomic Absorption Spectrometry (AAS) for Prrenjas bentonite and Wyoming montmorillonite. At increasing lead uptake, a higher reduction of hydration in interlayer space is observed by XRD on Wyoming montmorillonite. At the highest lead concentrations, X-ray Photoelectron Spectroscopy (XPS) analyses of the Prrenjas Bentonite reveal Pb sorption in a "non interlayer" site. TEM images of the same clay show an important size decreasing of microstructural units in relation to the lead sorption. On the contrary, the Mg-Wyoming montmorillonite is not modified.

Presumably, the "non interlayer lead" uptake results either from surface complexation at an edge site or from ionic exchange with edge-exposed octahedral magnesium. Both mechanisms could initiate at edge-to-face contacts and result in a breaking process of the microstructural units

Key words

lead, bentonite, microstructure, adsorption, cation exchange, XPS, TEM

1. Introduction

The usefulness of bentonites in several applications can be attributed to their high capability for sorbing heavy metal ions. In this respect, the interaction between toxic heavy metals and clay minerals is of great interest in environmental-pollution studies, waste management and soil science. Retainment of heavy metals is at the basis of geochemical barriers against aquatic pollutants (Brigatti et al., 1995). In this regard, smectites are playing an important role as components of geological landfill barriers e.g. as Geosynthetic Clay Liners (Bouazza, 2002). For a given smectite and fixed geometrical and hydrodynamical conditions, clay/solution interactions are controlled by the solution composition, in particular by ionic strength, pH and saturation state. These interactions result in various effects at different scales from nanoscopic (e.g. cation sorption with ion exchange; Sposito, 1984) to macroscopic (e.g. variation of hydraulic conductivity; Petrov et al., 1977, or shrink-swell behaviour; Tuller and Or, 2003).

A percolation experiment carried out by Jozja et al., (2003) with a natural (Mg, Ca)-bentonite from Prrenjas, Albania, and a lead nitrate (10^{-2} M) solution, until saturation by lead of the compacted clay, has shown a great increase, by a factor forty, of the permeability during lead uptake. It was only by a factor two with a Mg-exchanged Wyoming Na-montmorillonite (Jozja, 2003). The great differences observed with a same solution and similar amounts of lead suggest different relations between metal sorption and permeability variations for these two clays.

Thus, in order to explain the influence of elevated lead concentrations on the permeability increase of a (Mg, Ca)-bentonite, the aim of the present paper is to analyze microstructural modifications parallel to lead sorption. The general idea is to prepare samples of Prrenjas bentonite and reference Mg-exchanged Wyoming Na-montmorillonite equilibrated in suspension at different lead concentrations scattering in the range 0.01 to 10 mmol L^{-1} then to characterise lead fixation and the microstructure of clay aggregates. Solutions were analysed by Flame Atomic Absorption Spectrometry (F-AAS) and clay samples that had reacted with solutions were studied by X-ray diffraction (XRD), Transmission Electron Microscopy (TEM) and X-ray Photoelectron Spectroscopy (XPS). The results of these studies are then used to address two issues relating lead uptake with the clay microstructure:

- the fixation mechanisms of lead with special respect to “non interlayer” sorbed metal (XRD, F-AAS, XPS)

- the texture of clay aggregates and its variations after interaction with lead-rich solutions (TEM).

2. Materials and Methods

2.1. Samples

The bentonite used in this work is originating from the Prrenjas region (Albania). It is derived from supergene alteration of Mg-rich ultrabasic rocks followed by transport then sedimentation of alterites in lagoons during Holocene times. It is largely made up of a smectite (Jozja, 2003). In order to preserve the initial "natural" state of Prrenjas bentonite, no chemical treatment was carried out. The coarse fraction was removed by sedimentation in pure water. In addition to clays, the purified bentonite sample contains several impurities, mainly quartz (about 2%), and less than 1% of plagioclase and carbonate.

A Wyoming Na-montmorillonite (called SPV; Comptoir des Minéraux et Matières Premières, France; Auboiroux, 1998) was chosen as a reference material. As shown later, the main cation released during CEC determinations of the Prrenjas bentonite is Mg^{2+}. For this reason, the Wyoming Na-montmorillonite was transformed to the Mg-dominated form. Chemical composition of the two materials is presented in Table 1.

2.2. Clay mineralogy and physicochemical properties

XRD analyses were performed with a Nonius Diffractis 582 diffractometer, automated with an electronic device controlled by a Siemens Diffrac-AT system, using Cu Kα radiation (at 35 kV and 25 mA),. Characterisation of powders was carried out using both oriented air-dried samples and ethylene glycol solvated ones. Powder XRD patterns of Prrenjas bentonite indicate the predominance of smectite significantly affected by ethylene glycol solvation (17.55 Å) and are indicative of the presence of interstratified 1:1 phases. Although no illite peaks were detectable by XRD, K_2O contents would indicate the presence of illitic components. Otherwise, a study by Small Angle X-ray Scattering (Jozja, 2003) showed that the smectite phase of Prrenjas bentonite contains approximately 10% illite layers, in good agreement with K_2O contents indicated by chemical analysis. Moreover, the smectite peaks are broader than generally observed, suggesting the presence of illite in random interlayering with smectite (Jozja, 2003).

Clay samples were examined with a Philips CM 20 transmission electron microscope (TEM). To have a good transmission of the electron beam, the samples were prepared as ultra-thin sections. Investigations were carried out in the gel-like form (1.5 g H_2O per 1 g clay). For this purpose, and to perturb, as little as possible, the initial microstructural organisation of clay/water system, the sample internal water was substituted by a resin, using solvents (Tessier, 1984). TEM observations confirm the presence of smectite as the principal clay mineral and clarify the identity of 1:1 phases detected by XRD. There is a low percentage of antigorite (about 7%) and approximately 10% of kaolinite and halloysite. Minor chlorite is also detected.

Moreover, the smectite phase of the Prrenjas clay studied by TEM displays a distinct structure. Indeed, one can observe microstructural units largely consisting of an association of small particles, closely packed together, without inter-particle pore space. These microstructural units can be defined as microaggregates (Figure 1a). The mean size of microaggregates is 0.3 to 0.4 µm with a maximum size of about 0.7 µm. The particles that compose the microaggregates are small, with a lateral extension generally lower than 0.1 µm. They are associated not only face-to-face and edge-to-edge, but also edge-to-face. In addition, particles of Prrenjas clay are more or less rigid and are made of a small number of layers (statistically 14). In comparison, Wyoming Mg-montmorillonite was studied by TEM. Investigations show that the magnesium exchange of Wyoming Na-montmorillonite leads to a decrease of particle dimensions without modifying the typical texture of smectite (Figure 1b).

The most important physicochemical properties of Wyoming Mg-montmorillonite and Prrenjas bentonite are presented in Table 2. Cation Exchange Capacity (CEC) was determined using the cobaltihexamine method (Morel,1957) and related to the weight of calcinated clay. Cobaltihexamine ion concentration was measured by the colorimetric method, using a HITACHI U-1100 Spectrophotometer, at 473 nm. The CEC of Prrenjas sample is slightly inferior to that of the Wyoming clay. Solution analysis by F-AAS shows that about 80% of exchangeable sites are occupied by Mg^{2+} and 20% by Ca^{2+}. In fact, an evaluation of the nature of the layer charge was made using Hofmann and Klemen's procedure (Hofmann and Klemen, 1950). For Prrenjas bentonite about 45% of tetrahedral charge has been determined indicating, for this clay, a beidellitic character. External surface area (S_E) was determined by nitrogen adsorption using a Micromeritics ASIP 2000 apparatus and applying the BET equation. With the same operating procedure (drying at 105 °C, desorption under vacuum at 105 °C, multi-points method)

for the two samples, the surface area of 95.3 ± 1.2 $m^2.g^{-1}$ of Prrenjas bentonite, in comparison with Wyoming montmorillonite (surface area of 46.0 ± 1.1 $m^2\ g^{-1}$), suggests smaller particle size The total specific surface (S_T) was determined using the Ethylene Glycol Surface Method (Eltantawy and Arnold, 1974). The weight percentage of smectite layers of Prrenjas sample was evaluated about 80%, assuming a mean total surface area of respectively 140 and 750 $m^2\ g^{-1}$ for pure illite and smectite. Furthermore, permeability with pure water, obtained according to the generalised Darcy's law, using an oedometer device (Jozja, 2003), is in the range of 10^{-11} m s^{-1}, about ten times higher than that of the Wyoming Mg-montmorillonite (10^{-12} m s^{-1}) determined by the same technique.

2.3. Approximated structural formula

The structural formula of the Wyoming montmorillonite sample (in Ca-exchanged form) was previously determined by Auboiroux (1998) from chemical analysis and assuming that Ca, Na and K are in exchangeable sites :

$$\mathbf{(Ca_{0.188}Na_{0.003}K_{0.002})(Al_{1.56}Mg_{0.25}Fe_{0.18}Ti_{0.005})(Si_{3.91}Al_{0.09})O_{10}(OH)_2}$$

For Prrenjas bentonite, the difficulties due to compositional variability, sample heterogeneity (i.e., illite/smectite interlayering) and impurities, even in the finest clay-size fraction, complicate the determination of the true structural formula. In this case, a crystal-chemical formula of the 2:1 phase of Prrenjas bentonite was calculated from the chemical analysis of a Na-exchanged sample and also from hypotheses about the proportion of the additional phases (antigorite, kaolinite and halloysite) (Jozja, 2003). Moreover, an ideal structural formula was assigned to these additional phases.

In these conditions, the following structural formula, in which K corresponds to the minor interstratified illite component, was established:

$$\mathbf{(Na_{0.42}K_{0.09}Mg_{0.034}Ca_{0.009})(Fe^{3+}_{1.26}Al_{0.45}Mg_{0.24}Fe^{2+}_{0.006})(Si_{3.69}Al_{0.30})O_{10}(OH)_2}$$

Taking into account uncertainties, this structural formula is considered as the most reliable approximation. But, it is obvious that this result must be used with caution.

2.4. Experimental procedure

Suspensions of clays were made by adding 360 mg of clay to 100 ml of lead nitrate solutions, with different Pb concentrations in the range 10^{-5} M to 10^{-2} M, in a 250 mL centrifugation container closed with a sealing cap to limit interaction with atmospheric CO_2. Lead solutions were obtained by diluting, with ultra-pure water, a 10^{-2} M stock solution prepared from high grade lead nitrate (Merck). The pH was systematically measured. Depending on the metal concentration of the initial solution, it was found to be 5.7, for the lowest concentration and 3.8 for the highest one. In addition, the lead concentration of initial solutions was controlled by F-AAS using a HITACHI Z-8100 spectrophotometer with Zeeman background correction. Working curves were established with standards obtained by dilution of a 1000 mg L^{-1} commercial standard solution. Analytical accuracy is ± 1 % with detection limits varying from 0.01 mg L^{-1} for Na and Mg and 0.05 mg L^{-1} for K and Ca to 0.2 mg L^{-1} for Pb.

Initially, kinetic experiments were performed, with two initial Pb concentrations (10^{-4} M and 10^{-3} M), to make sure that the exchange duration is sufficient to reach an equilibrium state. Six runs (0.5, 1, 2, 4, 16 and 24 h) were selected. A stationary state was reached within 0.5 h, indicating that exchange phenomena were very fast. However, a larger run duration (16 h) was chosen.

To each initial Pb concentration there is a corresponding sample. The clay suspensions were shaken with an IKA HS 250 shaker during 16 h at room temperature (25°C). Then, the solid was separated from the solution by centrifugation during 20 minutes at 4500 rpm with a SV8-FIRLABO centrifuge. Pb, Mg and Ca concentrations were determined in equilibrium solutions using F-AAS. At the end of runs, the pH of the suspensions were systematically measured. The separated solid samples were rinsed with ultra-pure water using a filtration device, then air dried and reserved for studies by XRD, TEM and XPS.

For TEM observations of lead exchanged samples, the hydration phase has not been applied during the sample preparation, in order to minimise textural modifications and, to have a same object for other analysis techniques. In this case, the “voids” (water + air) are substituted with a resin by carrying out an inclusion.

XPS analyses were performed with an AEI ES 200B spectrometer using a magnesium anticathode. In this technique (Paterson and Swaffield, 1994) the proportion of emitted photoelectrons that may escape the solid without energy loss decreases exponentially with depth and may be considered negligible beyond three “mean free paths” (i. e. about

7 nm for silicates; Kuhr and Fitting, 1999; Jung et al., 2003). Samples were gently crumbled then put onto adhesive tape. The binding energy of $Pb_{4f7/2}$ photoelectrons was determined with reference to Si_{2p} photoelectrons with E_b = 102.7 eV (Wagner et al., 1978) rather than adventitious carbon because of the electrical insulator character of the samples. Quantitative results are expressed as atomic concentration ratios normalised to silicon. Sensitivity factors for quantitative analysis were previously determined from glasses of known composition. Uncertainties on atomic ratios can be estimated to ± 5% (Pb/Si) to ± 10% (for other ratios) since heavy elements, i.e. Pb, are more sensitive.

3. Results of clay-lead solutions interaction

3.1. Solution analyses

After lead exchange, the pH of solutions is in range 7.3 to 4.6 for the highest lead concentrations. Figure 2 displays Pb amounts (mmol g^{-1}) sorbed by the clay and amounts of cations released in solution for Wyoming Mg-montmorillonite and Prrenjas bentonite. A good agreement between sorbed lead and the sum of released cations is noticed. For Wyoming Mg-montmorillonite, the results are similar to those obtained by Auboiroux et al., (1996) for the Ca-exchanged form. In both samples of Wyoming clay, the plateau value is lower than the CEC value determined by the cobaltihexamine method. A good capacity of lead retention is also observed for Prrenjas bentonite with a plateau value slightly higher than the CEC.

3.2. X-Ray Diffraction patterns

The initial and Pb-exchanged samples were analysed by XRD to observe the evolution of the d_{001} reflection with an increasing lead content in clay (Figure 3). Diffractograms of Wyoming Mg-montmorillonite and Prrenjas bentonite show that the lead exchange results in a shift of the peak to higher angles. Moreover, for Prrenjas bentonite a broadening of the peak is clearly observed while, for Wyoming Mg-montmorillonite, the peak remains narrow except at the concentration of 2 mmol L^{-1} where two peaks are found. The d_{001} value of the initial Prrenjas clay is 15.23 Å while it is 15.11 Å for the Wyoming Mg-montmorillonite. Figure 4 shows the evolution of d_{001} with increasing lead concentrations. For both materials, the d_{001} values decrease when the concentration

of lead is higher than about 1 mmol L^{-1}. This effect is enhanced in the Pb-exchanged Wyoming samples (d_{001} = 12.70 Å) in comparison with Prrenjas bentonite (d_{001} = 13.59 Å).

3.3. TEM observations

For both materials, the TEM examination was carried out for Pb-exchanged samples corresponding to lead solution concentrations of 0.8 mmol L^{-1} and 10 mmol L^{-1}. TEM observations of Wyoming samples do not show important structural modifications, at the investigated level, even by interaction with 10 mmol L^{-1} solution (Figure 5a). However, a face-to-face re-association of particles seems to occur to form thicker units. In contrast, TEM investigations of the Pb-exchanged Prrenjas bentonite sample, related to the 10 mmol L^{-1} solution, reveal an important size decrease of the microstructural units with respect to the initial structure (Figure 5b). The mean size of microaggregates is about 0.2 µm while the lateral extension of the associated particles is not significantly modified (predominantly lower than 0.1 µm). Moreover, a number of single particles are formed evenly throughout the area as can be seen in Figure 5b. At this concentration of 10 mmol L^{-1}, a lead-rich zone, probably made of lead precipitates (carbonates ?), was locally observed. These structural modifications are far less important at the concentration of 0.8 mmol L^{-1}; only a limited size decrease of microstructural units being noticed. Moreover, at this lower concentration, the precipitation of lead compounds has never been observed.

3.4. XPS analysis

The binding energy of the $Pb_{4f7/2}$ photoelectrons is 139.4 ± 0.2 eV for Prrenjas sample and 139.8 ± 0.2 eV for Wyoming Mg-montmorillonite. Due to the charge of layers these values are largely higher than that of the reference lead nitrate compound (138.5 eV). Moreover, the lower binding energy for Prrenjas sample can be attributed to the higher d_{001} spacing when compared to Wyoming Mg-montmorillonite (Dutta et al., 1999).

Based on XPS data, Figure 6 indicates the variation of the Pb/Si atomic ratio as a function of lead concentration of initial solution in mmol L^{-1}. The Pb/Si atomic ratio increases with the initial Pb content of the solution until it reaches, at 6 mmol L^{-1}, a plateau value of about 0.11. Furthermore, a slight inflexion of the curve is suspected at 1 mmol L^{-1}. The XPS data for the Wyoming Mg-montmorillonite are also reported in this Figure. Initial Pb/Si values are mixed up with those of Prrenjas sample. The plateau

value close to 0.065, significantly lower than for Prrenjas bentonite, is reached at about 2 mmol L^{-1}.

4. Discussion and conclusion

The main characteristics of Prrenjas smectite, as determined by different methods of investigation, can be summarised as follows: i) significant magnesium is present in the octahedral layer in association with aluminium and iron; ii) magnesium and secondarily calcium are the main cations exchanged during CEC determinations and Pb uptake experiments; iii) 10% of illite is interlayered with the smectite phase; iv) microstructural units are composed of closely packed clay particles made of 10 to 15 stacked platelets. Concerning the magnesium content, Touret et al., (1990) and Churchman et al., (2002) have shown that magnesium-rich smectites are different from ordinary bentonites with, in particular, very small particles.

In smectites, sorbed metals (Fletcher and Sposito, 1989) form complexes either in the interlayer space to counterbalance the permanent negative charge of the layer (outer-sphere adsorption) or on the hydroxyl edge sites where the crystal structure is interrupted (inner-sphere adsorption). X-ray absorption spectroscopy permits to distinguish between the two sites from their different local atomic structures (LAS) when heavy metals such as lead (Strawn and Sparks, 1999), cobalt (Schlegel et al., 1999) or copper (Morton et al., 2001) are sorbed by smectites. With respect to lead, XAFS results (Strawn and Sparks, 1999) indicate at low ionic strength and variable acid pH an outer sphere complexation with the LAS surrounding the adsorbed Pb similar to the LAS surrounding aqueous Pb^{2+}. At elevated ionic strength and slightly acidic pH, the LAS is characteristic of inner-sphere complexation. By varying the pH solution and the concentration of electrolyte, samples with heavy metal dominantly located at interlayer or edge sites may be prepared (Morton et al. 2001). Both adsorption complexes may be present in the same sample, depending on pH and ionic strength (Strawn and Sparks, 1999). In addition to chemical parameters, the size and morphology of smectite particles clearly plays a role with respect to the relative importance of edge sites. An elevated ratio (basal area)/(thickness), typical of Wyoming montmorillonite, will favour the relative importance of interlayer sites. A third type of sorption, the replacement of edge-exposed octahedral Mg is possible. It has been proposed to partly explain the fixation of copper and zinc on the surface of sepiolite (Vico, 2003). It has been documented during

uptake experiments of cobalt by hectorite, a magnesian smectite (Schlegel et al., 1999). This process results in equimolar metal sorption and Mg release. If it is relevant in the case of the magnesium-rich Prrenjas bentonite, edge-exposed Mg is included in the CEC and lead may be fixed at these sites after ionic exchange. An indirect consequence of the exchange of interlayer hydrated cations (alkaline or alkaline earth elements) with aqueous lead at an elevated concentration is a decrease of the basal spacing of a smectite related to a decrease of the number of water layers. This fact underlines the role of lead on the swelling properties of bentonites (Brigatti *et al.,* 1995; Auboiroux *et al,*. 1996). More generally it is admitted (Siantar and Fripiat, 1995; Brindley and Brown, 1980) that when d_{001} is about 15.5 Å, one has a two-water-layer hydrate, when it is about d_{001} = 12.5 Å there is only one water layer. When it scatters in the range 12.5 to 15.5 Å one has an interstratification of one and two-water-layer hydrates. Considering Prrenjas and Wyoming clay materials, interstratification is the general case. At the higher lead concentrations, the two different clays display distinct hydration states. With a maximal Pb uptake the Wyoming sample presents only one water layer, while the Prrenjas bentonite remains in an interlayering one/two-water-layer. This result suggests that, in the Prrenjas clay, at concentrations higher than 1 mmol L^{-1}, less lead has been trapped in an interlayer site with respect to the Wyoming Mg-montmorillonite. On the contrary, in the 1 to 10 mmol L^{-1} range, Figure 2 indicates similar amounts of total lead fixed by both materials. Accordingly, a non interlayer sorption site has to be involved, at elevated concentrations and ionic strengths, in the Prrenjas bentonite.

Clay minerals, as a result of their planar layered structure, are easily studied by XPS before and after metal uptake (Adams and Evans, 1979; Davidson and McWhinnie, 1991; Auboiroux et al., 1998; Gier and Johns, 2000). XPS data are useful to put in evidence the lack or existence of ionic exchanges. The Al/Si and Fe/Si atomic ratios measured on Prrenjas bentonite do not vary significantly whatever the initial Pb concentration in the solution. They are respectively 0.35 ± 0.04 and 0.28 ± 0.03 for the ten Pb-exchanged samples in comparison with 0.38 and 0.29 for the initial sample. Accordingly, the possibility of an exchange of Pb with Al or Fe may be discarded. Due to the chemical composition of Prrenjas sample the decrease of the Mg/Si atomic ratio during the exchange is relatively low from about 0.19 to 0.14. In Figure 7, the sum of Pb/Si, Mg/Si and Ca/Si atomic ratios is plotted versus the amount of sorbed Pb, determined from solutions analysis. The constancy of this sum is consistent with ionic exchange of Pb with Mg and Ca. It is the case for Wyoming Mg-montmorillonite and, at low concentrations, for Prrenjas bentonite. But, for the latter, at the highest Pb concentrations, a slight but significant discrepancy is noticed in agreement with the

existence of an additional sorption process. Figure 8 plots, for Wyoming Mg-montmorillonite and Prrenjas bentonite, the Pb/Si atomic ratio of the solid, obtained by XPS, as a function of the amount of lead fixed by the material. The results for a Wyoming Ca-montmorillonite (Auboiroux, 1998) are also reported. A linear trend can be noticed at the lowest concentrations. When lead uptake results from an exchange with interlayer cations, the Pb/Si atomic ratio determined by XPS increases with the concentration of sorbed lead. This relation is linear if the atomic lead concentration by volume is identical within the four or five surface layers (corresponding to an analysed depth of about three mean free paths of $Pb_{4f7/2}$ and Si_{2p} photoelectrons) and in the bulk sample. Indeed, on the one hand, this volume concentration, which is a function of the basal spacing, is obviously proportional to the molar concentration of sorbed lead. On the other hand, the atomic concentration of silicon by volume monitors the basal spacing variation effect. Consequently, the Pb/Si atomic ratio is independent of the degree of swelling and proportional to the molar concentration of sorbed lead. As indicated in Figure 8, a good linear trend is observed with Wyoming montmorillonite at any lead concentration. For the lowest lead concentrations (up to about 1 mmol L^{-1}), a linear relationship is also noticed for Prrenjas bentonite. Silicon distribution being nearly the same within tetrahedral layers of different smectites, the two trends are nearly superimposed. At higher concentrations the elevated values of Pb/Si ratios, well above the linear trend, suggest an excess Pb sorption on the Prrenjas clay somewhere else than in the interlayer space (“non interlayer lead”).

Two hypotheses may be formulated to explain this result. The first one is the fixation of lead by surface complexation at edge sites and (or) by ionic exchange with edge-exposed magnesium. The second hypothesis is the presence of a Pb-rich precipitated phase (Siantar and Fripiat, 1995). Although samples studied by TEM are not statistically representative of the bulk, the rare appearance of Pb-rich precipitates can be noticed. Thus, after Pb exchange the pH is increasing due to Mg (and Ca) concentration in the solution. However, for the highest initial lead concentration the pH remains under 5. In these conditions, calculations using solubility products of lead hydroxide [$\log(K_{sp}) = -19.5$] and lead carbonate [$\log(K_{sp}) = -13.1$] indicate that only (ageing) 10^{-2} M experiments could lead to carbonate precipitation. On the other hand, if the sample is not well rinsed, lead-compound precipitates can be observed on dried samples in relation to increase ionic concentrations. They would hardly be detected by XPS, because their apparent area, as “seen” by impinging X rays, would be small.

In contrast, one may consider small size particles made of 10-15 stacked platelets with a lateral extension of 50 to 150 nm (Figure 5, b). Lead atoms located at edge surface, as well as

in substitution to edge-exposed Mg will be easily detected by XPS (Figure 9) mostly because the corresponding photoelectrons are directly emitted from the surface without absorption. TEM investigations show the importance of the effect on the size reduction (Figure 10) of microstructural units of the Prrenjas bentonite after interaction with 10 mmol L^{-1} solution. The process is only incipient with 0.8 mmol L^{-1} solution. Moreover from Figure 8 ”non interlayer lead” is detected when total fixed lead is higher than about 0.3 mmol g^{-1}, corresponding to an initial concentration higher than about 0.2 mmol L^{-1} (Figure 6). Accordingly, at a 10 mmol L^{-1} concentration, the size reduction of microstructural units may be correlated with lead uptake in a non interlayer site. Presumably, lead uptake results either from surface complexation at an edge site or from ionic exchange with edge-exposed octahedral magnesium. Both mechanisms probably initiate at edge-to-face contacts, which are especially numerous in Prrenjas bentonite, leading to the disassociation of the particles forming the microstructural units.

This conclusion has been established with clay suspensions but probably the breaking process of clay aggregates in smaller units also occurs when clay is compacted. The texture modification of the clay material, resulting from the disassociation process, could favour the percolation of water by pore enlargement and creation of new percolation paths. Thus, this process, at the scale of microaggregates, is probably the cause of the enhancing permeability of compacted Prrenjas bentonite (Jozja et al., 2003) observed, with a high lead concentration solutions, at lead saturation.

References

Adams, J.M. & Evans, S. (1979) - Exchange and selective surface uptake of cations by layered silicates using X-ray photoelectron spectroscopy (XPS). *Clays and Clay Minerals*, **27**, 248-252.

Auboiroux, M., Baillif, P., Touray, J.C. & Bergaya, F. (1998) - XPS analysis at constant ionic strength of Ca-Cd and Ca-Pb exchanges on a Ca-montmorillonite. *Comptes Rendus de l'Académie des Sciences - Series IIA - Earth and Planetary Science*, **327**, 727-730.

Auboiroux, M. (1998) - Affinité de différents cations métalliques (Co^{2+}, Ni^{2+}, Cu^{2+}, Zn^{2+}, Cd^{2+}, Pb^{2+}) pour une montmorillonite calcique. Expérimentation et applications. Ph.D. Thesis, Univ. Orléans, France, 304 pp.

Auboiroux, M., Baillif, P., Touray, J.C. & Bergaya, F. (1996) - Fixation of Zn^{2+} and Pb^{2+} by a Ca-montmorillonite in brines and dilute solutions: Preliminary results. *Applied Clay Science*, **11**, 117-126.

Bouazza, A. (2002) - Geosynthetic clay liners. *Geotextiles and Geomembranes*, **20**, 3-17.

Brigatti, M. F., Corradini, F, Franchini, G. C., Mazzoni, S., Medici, L. & Poppi L. (1995) - Interaction between montmorillonite and pollutants from industrial waste-waters: exchange of Zn^{2+} and Pb^{2+} from aqueous solutions. *Applied Clay Science*, **9**, 383-395.

Brindley, G. W. & G. Brown (1980) Crystal structures of Clay Minerals and Their Identification. Mineralogical Society, London, 495 pp.

Churchman, G. J., Askary, M., Peter, P., Wright, M., Raven, M. D.& Self, P. G. (2002) - Geotechnical properties indicating environmental uses for an unusual Australian bentonite. *Applied Clay Science*, **20**, 199-209.

Davison, N. & McWhinnie, W.R. (1991) - X-Ray Photoelectron Spectroscopic Study of Cobalt (II) and Nickel(II) Sorbed on Hectorite and montmorillonite. *Clays and Clay Minerals*, **39**, 22-27.

Dutta, N.C., Iwasaki, T., Ebina, T. & Hayashi, H. (1999) - A Combined X-Ray Photoelectron and Auger Electron Spectroscopic Study of Cesium in Variable-Charge montmorillonites. *Journal of Colloid and Interface Science*, **216**, 161-166.

Eltantawy, I.M. & Arnold, P.M. (1974) - Ethyleneglycol sorption by monoionic montmorillonites. *J. of Soil Science*, **25**, 99-110.

Fletcher, P. & Sposito, G. (1989) - The chemical modelling of clay-electrolyte interactions for montmorillonite. *Clay Minerals*, **24**, 375-391.

Gier, S. & Johns, W.D. (2000) - Heavy metal-adsorption on micas and clay minerals studied by X-ray photoelectron spectroscopy. *Applied Clay Science*, **16**, 289-299.

Hofmann, U. & Klemen, R. (1950) - Verlust der Austauschkapacität vor Lithiumionen an Bentonit durch Erhitzung. *Z. Anorg. Chem.*, **262**, 95-99.

Jozja, N. (2003) - Etude de matériaux argileux albanais. Caractérisation « multiéchelle » d'une bentonite magnésienne. Impact de l'interaction avec le nitrate de plomb sur la perméabilité. Ph.D. Thesis, Univ. Orléans, France, 245 pp. : http://tel.ccsd.cnrs.fr/documents/archives0/00/00/37/40/index_fr.html

Jozja, N., Baillif, P., Touray, J.C., Pons, C.H., Muller, F. & Burgevin, C. (2003) - Impacts « multi-échelle » d'un échange (Mg,Ca)-Pb et ses conséquences sur l'augmentation de la perméabilité d'une bentonite: Multiscale impacts of a (Mg,Ca)-Pb exchange on the permeability increase of a bentonite. *Comptes Rendus Geosciences*, **33**, 729-736. : http://hal.ccsd.cnrs.fr/ccsd-00069451

Jung, R., Lee, J. C, Orosz, G. T., Sulyok, A., Zsolt, G. & Menyhard, M. (2003) - Determination of effective electron inelastic mean free paths in SiO_2 and Si_3N_4 using a Si reference. *Surface Science*, **543**, 153-161.

Kuhr, J.C. & Fitting, H.J. (1999) - Monte Carlo simulation of electron emission from solids, *Journal of Electron Spectroscopy and Related Phenomena*. **105**, 257-273.

Morel, M. (1957) Observations sur la capacité d'échange et les phénomènes d'échange dans les argiles. *Bull. Gr. Fr. Argiles*, **12**, 3-8.

Morton, J.D., Semrau, J.D. & Hayes, K.F. (2001) - An X-ray absorption spectroscopy study of the structure and reversibility of copper adsorbed to montmorillonite clay. *Geochimica et Cosmochimica Acta*, **65**, 2709-2722.

Paterson, E. & Swaffield, R. (1994) - X-ray photoelectron spectroscopy. In : Spectroscopic and chemical determination methods. Chapman & Hill, London, 226-259.

Petrov, R.J., Rowe, R.K. & Quigley, R.M. (1997) - Selected factors influencing GCL hydraulic conductivity. *Journal of Geotechnical and Geoenvironmental Engineering*, **123**, 683-695.

Schlegel, M.L., Charlet, L. & Manceau, A. (1999) - Sorption of Metal Ions on Clay Minerals: II. Mechanism of Co Sorption on Hectorite at High and Low Ionic Strength and Impact on the Sorbent Stability. *Journal of Colloid and Interface Science*, **220**, 392-405.

Siantar, D.P. & Fripiat, J.J. (1995) - Lead Retention and Complexation in a Magnesium Smectite (Hectorite). *Journal of Colloid and Interface Science*, **169**, 400-407.

Sposito, G. (1984) - *The Surface Chemistry of Soils*, Oxford University Press, New York, 234 pp.

Strawn, D.G. & Sparks, D.L. (1999) - The Use of XAFS to Distinguish between Inner- and Outer-Sphere Lead Adsorption Complexes on montmorillonite. *Journal of Colloid and Interface Science*, **216**, 257-269.

Tessier, D. (1984) - Etude expérimentale de l'organisation des matériaux argileux. Hydratation, gonflement et structure au cours de la dessiccation et de la réhumectation. Ph.D. Thesis, Univ. Paris VII, France, 361 pp.

Touret, O., Pons, C.-H., Tessier, D.& Tardy, Y. (1990) - Etude de la répartition de l'eau dans les argiles saturées Mg^{2+} aux fortes teneurs en eau. *Clay Minerals*, **25**, 217-233.

Tuller, M. & Or, D. (2003) - Hydraulic functions for swelling soils: pore scale considerations. *Journal of Hydrology*, **272**, 50-71.

Vico, L.I. (2003) - Acid-base behaviour and Cu^{2+} and Zn^{2+} complexation properties of the sepiolite/water interface. *Chemical Geology*. **198**, 213-222.

Wagner, C.D., Riggs, W.M., Davis, L.E., & Moulder, J.F. (1978) - *Handbook of X-ray photoelectron spectroscopy*. Perking-Elmer Corporation, Physical Electronics Division, Eden Prairie, 190 pp.

Table captions

Table1. Chemical composition (in %) of Wyoming montmorillonite (Ca-exchanged form) and purified Prrenjas bentonite.

Table 2. Physicochemical properties of Wyoming Mg-montmorillonite and Prrenjas bentonite after separation of the coarsest impurities.

	SiO_2	Al_2O_3	Fe_2O_3	FeO	MgO	TiO_2	MnO	CaO	Na_2O	K_2O	P_2O_5	L.O.I.
Wyoming	54.23	19.37	3.25*		2.27	0.13	0.01	2.41	0.02	0.02	0.05	18.20
Prrenjas	46.33	9.95	14.23	0.43	9.08	0.43	0.19	0.5	0.18	0.83	0.03	17.77

* as total Fe_2O_3

Table1. Chemical composition (in weight %) of Wyoming montmorillonite (Ca-exchanged form) and purified Prrenjas bentonite.

Prrenjas Bentonite					
Total Specific Surface (S_T)	600 $m^2 g^{-1}$				
External Surface Area (B.E.T)	95.4 $m^2 g^{-1}$				
Cation Exchange Capacity (CEC)	82 meq per 100g of calcinated clay				
Tetrahedral substitutions	45 %				
Exchangeable Cations		Mg^{2+}	Ca^{2+}	K^+	Na^+
	%	78	18	3	1
Wyoming Mg-Montmorillonite					
Total Specific Surface (S_T)	766 $m^2 g^{-1}$				
External Surface Area (B.E.T)	46 $m^2 g^{-1}$				
Cation Exchange Capacity (CEC)	96 meq per 100g of calcinated clay				
Tetrahedral substitutions	24 %				

Table 2. Physicochemical properties of Wyoming Mg-montmorillonite and Prrenjas bentonite after separation of the coarsest impurities.

Figure captions

Figure 1: a) TEM image of initial Prrenjas bentonite showing a microaggregate (M) between two arrows; b) TEM image of initial Wyoming Mg-montmorillonite showing two particles (P).

Figure 2. Amounts of Pb fixed and cations released as function of Pb concentration in equilibrium solution: a) Prrenjas bentonite; b) Wyoming Mg-Montmorillonite.

Figure 3. X ray Diffraction patterns of initial and lead exchanged clay samples: a) Prrenjas Bentonite; b) Wyoming Mg-sample.

Figure 4. Variation of basal spacing d_{001} versus initial lead concentration for Wyoming Mg-montmorillonite and Prrenjas bentonite.

Figure 5: a) TEM image of Wyoming Mg-montmorillonite treated with 0.01M $Pb(NO_3)_2$ solution. b) TEM image of Prrenjas bentonite treated with 0.01M $Pb(NO_3)_2$.solution with numerous little particles.

Figure 6. Variation of Pb/Si atomic ratio, determined by XPS, as function of lead concentration in the initial solution for: Wyoming Mg-montmorillonite (Wy-Mg) and Prrenjas bentonite (Prr).

Figure 7. Sum of Pb/Si, Mg/Si and Ca/Si atomic ratios, determined by XPS, versus to the amount of Pb fixed in the clay for: Wyoming Mg-montmorillonite (Wy-Mg) and Prrenjas bentonite (Prr).

Figure 8. Variation of Pb/Si atomic ratio, determined by XPS, as function of the amount of Pb fixed in the clay for: Wyoming Mg-montmorillonite (Wy-Mg), Wyoming Ca-montmorillonite (Wy-Ca) and Prrenjas bentonite (Prr).

Figure 9. Schematic representation of the microstructural units of Prrenjas bentonite, with numerous edge-face associations of particles, showing the significance of edge surfaces for XPS analysis.

Figure 10. Size classes (in %) of microstructural units of Prrenjas bentonite before and after interaction with 10 mmol L^{-1} lead solution.

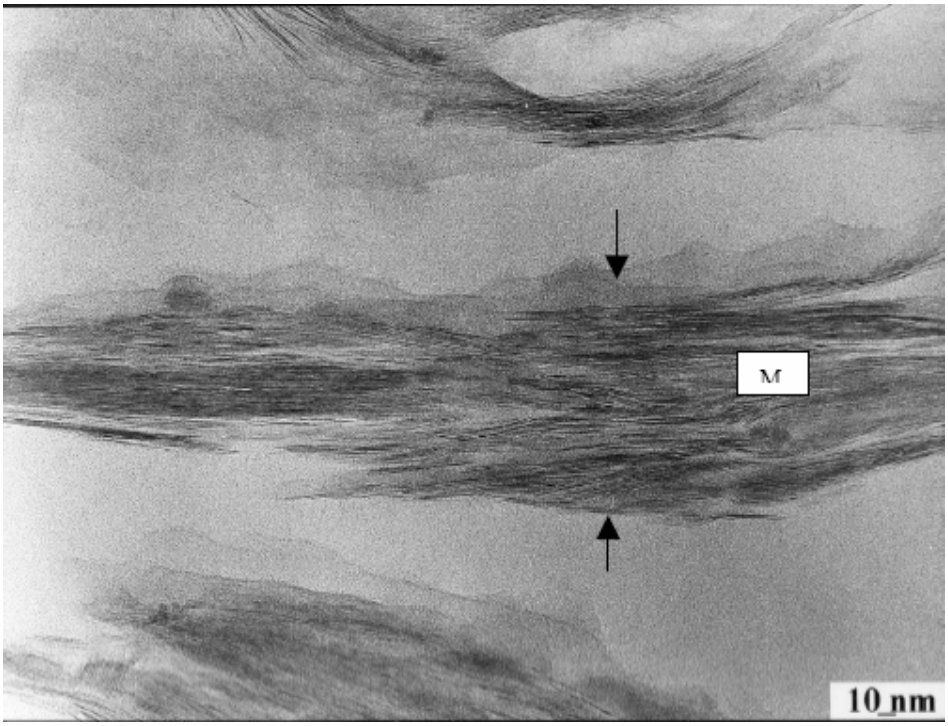

Figure 1. a) TEM image of initial Prrenjas bentonite showing a microaggregate (M) between two arrows;

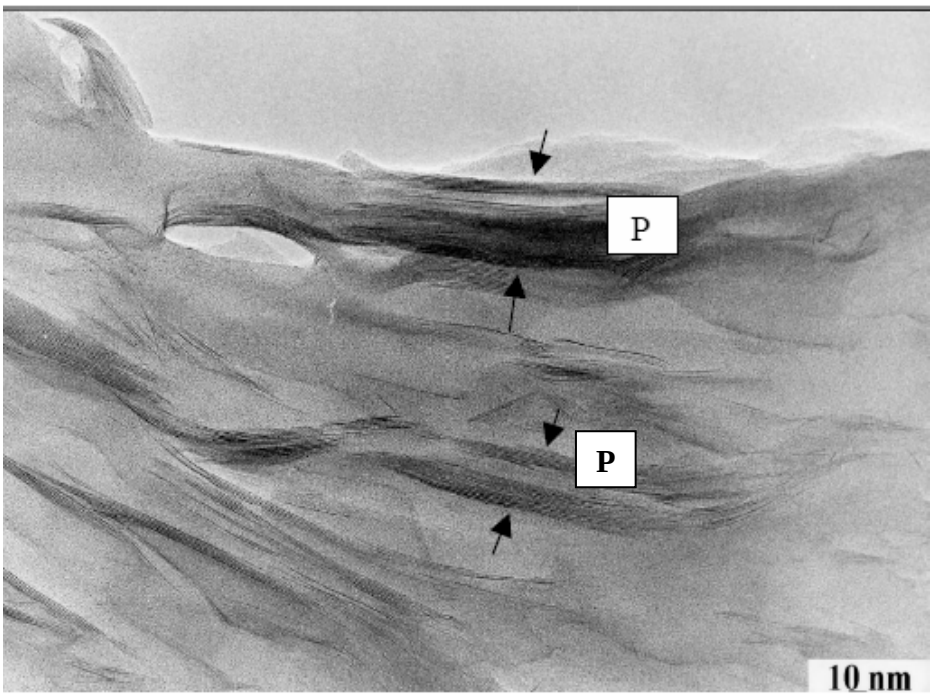

Figure 1. b) TEM image of initial Wyoming Mg-montmorillonite showing two particles (P).

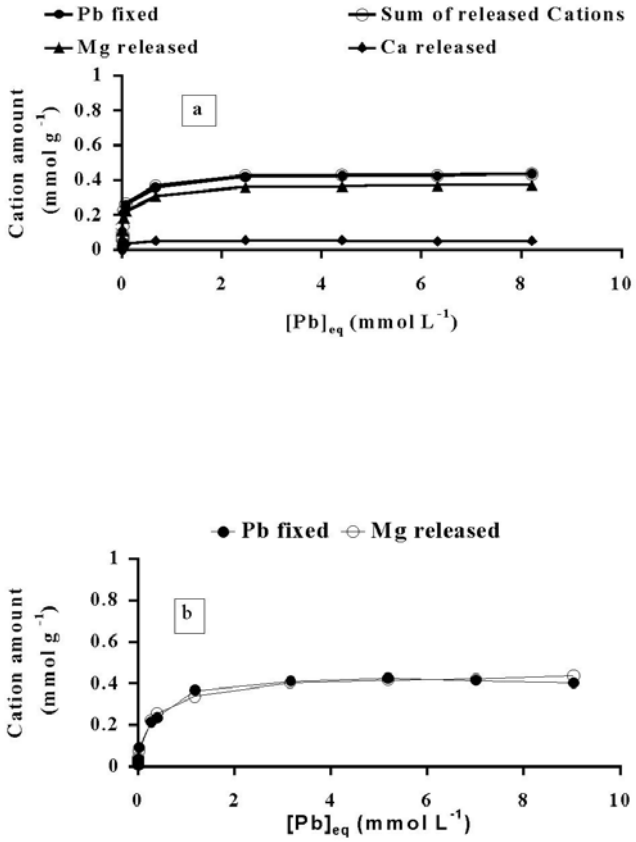

Figure 2. Amounts of Pb fixed and cations released as function of Pb concentration in equilibrium solution: a) Prrenjas bentonite; b) Wyoming Mg-Montmorillonite.

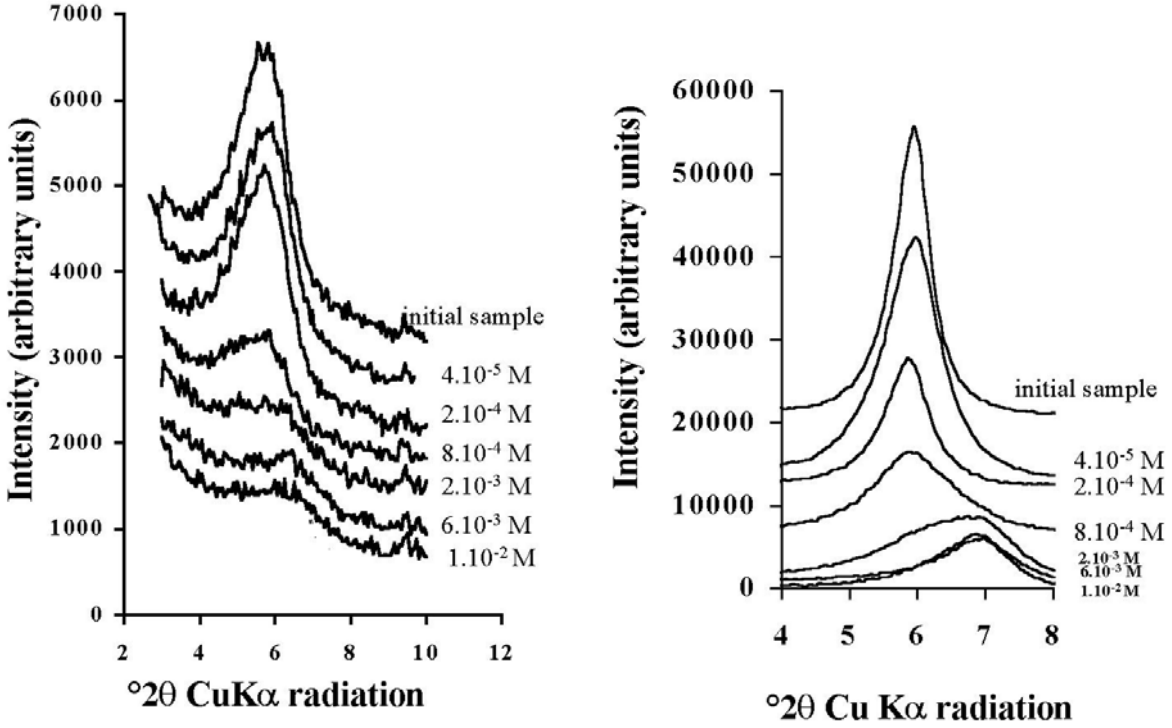

Figure 3. X ray Diffraction patterns of initial and lead exchanged clay samples: a) Prrenjas Bentonite; b) Wyoming Mg-sample.

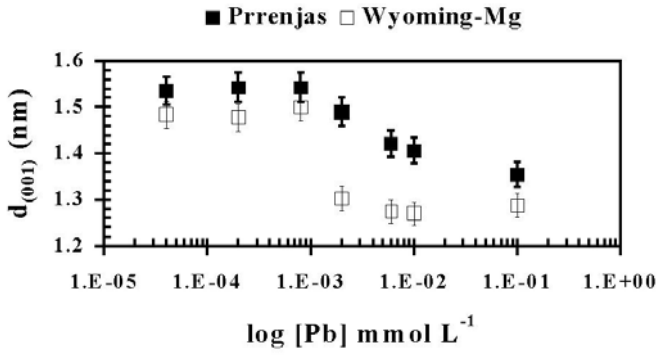

Figure 4. Variation of basal spacing d_{001} versus initial lead concentration for Wyoming Mg-montmorillonite and Prrenjas bentonite.

Figure 5. a) TEM image of Wyoming Mg-montmorillonite treated with 0.01M $Pb(NO_3)_2$.solution.

Figure 5. b) TEM image of Prrenjas bentonite treated with 0.01M $Pb(NO_3)_2$.solution with numerous little particles.

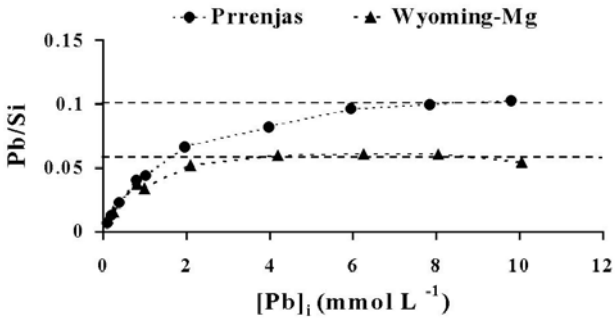

Figure 6. Variation of Pb/Si atomic ratio, determined by XPS, as function of lead concentration in the initial solution for: Wyoming Mg-montmorillonite and Prrenjas bentonite.

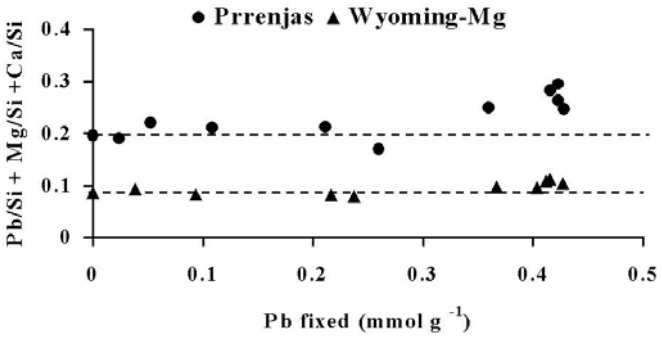

Figure 7. Sum of Pb/Si, Mg/Si and Ca/Si atomic ratios, determined by XPS, versus to the amount of Pb fixed in the clay for: Wyoming Mg-montmorillonite and Prrenjas bentonite.

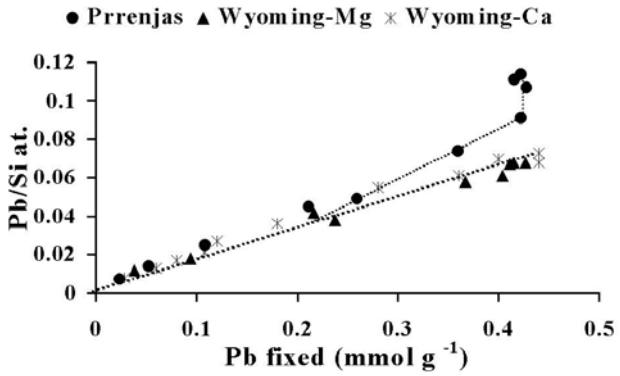

Figure 8. Variation of Pb/Si atomic ratio, determined by XPS, as function of the amount of Pb fixed in the clay for: Wyoming Mg-montmorillonite, Wyoming Ca-montmorillonite and Prrenjas bentonite.

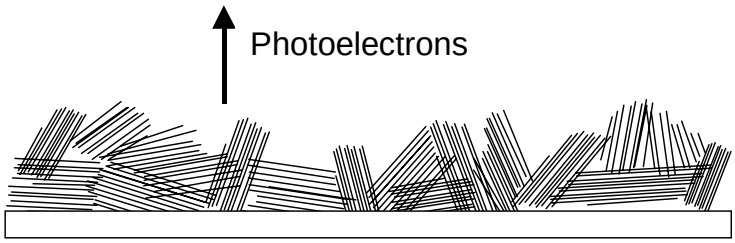

Figure 9. Schematic representation of the microstructural units of Prrenjas bentonite, with numerous edge-face associations of particles, showing the significance of edge surfaces for XPS analysis.

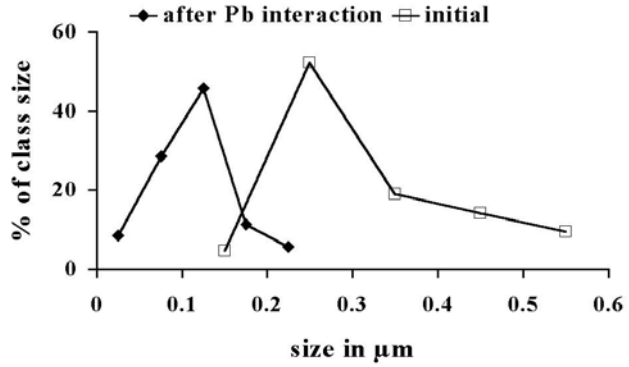

Figure 10. Size classes (in %) of microstructural units of Prrenjas bentonite before and after interaction with 10 mmol L^{-1} lead solution.